Nitrogen atom energy distributions in a hollow-cathode planar sputtering magnetron

Zhehui Wang*
Los Alamos National Laboratory, Los Alamos, New Mexico 87545

Samuel A. Cohen
Plasma Physics Laboratory, Princeton University, P.O. Box 451, Princeton, New Jersey 08543

David N. Ruzic
Department of Nuclear, Plasma and Radiological Engineering, University of Illinois, Urbana, Illinois 61801

M. J. Goeckner
Electrical Engineering Program, Plasma Science Laboratory, P.O. Box 830688 M/S EC33, University of Texas at Dallas, Dallas, Texas 75083

(Received 7 June 1999; revised manuscript received 30 September 1999)

Energy distributions of nitrogen atoms (N) in a hollow-cathode planar sputtering magnetron were obtained by use of optical emission spectroscopy. A characteristic line, N I 8216.3 Å, well separated from molecular nitrogen emission bands, was identified. Jansson's nonlinear spectral deconvolution method, refined by minimization of χ_w^2, was used to obtain the optimal deconvolved spectra. These showed nitrogen atom energies from 1 eV to beyond 500 eV. Based on comparisons with VFTRIM computer code results, it is proposed that the energetic N's are generated from N_2^+ ions after these ions are accelerated through the sheath and dissociatively reflect from the cathode.

PACS number(s): 52.40.Hf, 51.70.+f, 52.20.Hv, 52.25.Rv

I. INTRODUCTION

Neutralization is likely when an ion backscatters from a metal surface. Many experiments have studied backscattering for ion energies above a few hundred eV. At somewhat lower impact energies, 5–100 eV, Cutherbertson *et al.* [1] measured reflected-atom energy distributions for atomic ions backscattering as neutrals. Knowledge of reflected-atom energy distributions in the range 1–500 eV is essential for understanding basic ion-surface interactions, thin-film deposition processes, plasma-dust interactions, and Langmuir-probe operation.

Molecular ion species bombardment of surfaces is a more complex phenomenon, important in many atmospheric plasmas, e.g., spacecraft reentry, and many laboratory plasmas, e.g., the deposition of TiN or Al_2O_3 compound films. Computational methods [2] widely used to model the reflected-atom energy distribution for atomic bombardment have been less commonly applied to molecule backscattering because of the increased complexity and lack of experimental data to compare with the models.

In many laboratory plasmas, the electron temperature is only few eV and the ionization fraction less than 1%. Under such conditions, biatomic molecule (H_2, N_2, etc.) discharges usually contain both atomic (H^+,N^+) and molecular (H_2^+,N_2^+) ions. Both types of ions contribute to the reflected atom flux, the latter via fragmentation upon impact. This paper reports on the atomic-N energy distribution in a hollow-cathode planar sputtering magnetron (HCPM) [3]. In this paper we argue that the energetic N atoms observed are due to dissociative reflection of molecular ions which impact the cathode.

Nitrogen-atom energy distributions were obtained using optical emission spectroscopy (OES) wherein plasma electrons excite atomic and molecular species which then spontaneously decay, emitting visible-wavelength photons. OES has been used to characterize the species in plasma and to measure electron density, electron temperature T_e [4], and electron energy distribution function (EEDF), and ion and atom densities [5] and temperatures. Here we report on its application to the measurement of atomic-N energy distribution in a sputtering magnetron.

The ability to observe weak emission from backscattered nitrogen atoms arises from the fact that in a molecular nitrogen discharge the background light is due primarily to molecular nitrogen. Therefore, the background light near atomic-N lines *may* be greatly reduced and we *may* then be able to see a relatively weak signal due to the backscattered N atoms. Finding a spectral region where molecular emission is weak is actually quite a task.

In this paper we also describe the effects on the spectra of operational parameters, such as cathode material, bias voltage, and gas pressures, and also the heating of the ambient gas by backscattered atoms. The experimental data are compared with a numerical model (VFTRIM) [6] of backscattering. VFTRIM code is a Monte Carlo binary collision code. It simulates the particle-surface interaction process using a fractal model for the surface. Physical processes such as reflection (in which we are most interested), absorption, sputtering, etc., are simulated. Based on this study, the mechanism for generating energetic atomic N in a molecular nitrogen discharge is proposed.

*Electronic address: zwang@lanl.gov

 ©2000 The American Physical Society

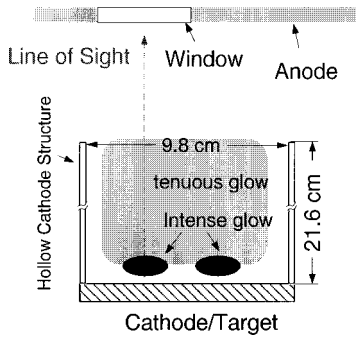

FIG. 1. Dimensions of the HCPM configuration and detection line of sight.

II. EXPERIMENT

Experiments were carried out on a hollow-cathode planar sputtering magnetron; see Fig. 1. Details of the operation of a HCPM can be found in earlier papers [3,7]. A negative dc bias (300–1500 V) is placed on the cathode structure. Ions impact there, ejecting secondary electrons which are accelerated through the cathode sheath. Within the plasma these electrons cause ionization events, replenishing the loss of ions to the cathode [8]. In brief, the HCPM acts much like a classical glow discharge, but with more efficient use of the energy of the ejected electrons because of the hollow cathode geometry and the magnetic field.

A schematic of the light detection setup is shown in Fig. 2. An Acton research SP500 spectrometer (0.5-meter focal length, Czerny-Turner type) with 1200 g/mm grating was used. The detector was a Hamamatsu R636-10 photomultiplier tube (PMT), which has high quantum efficiency in the region of interest, near 8000 Å. Cooling of the PMT was necessary to reduce its dark current by a factor of 100, thereby increasing the signal-to-noise ratio. When obtaining a high-resolution line profile, the spectrometer was scanned at a rate of 1 Å/min to provide a long exposure.

Using a the 826.45-nm line emitted from an argon Geissler tube, the instrumental width of the spectrometer was

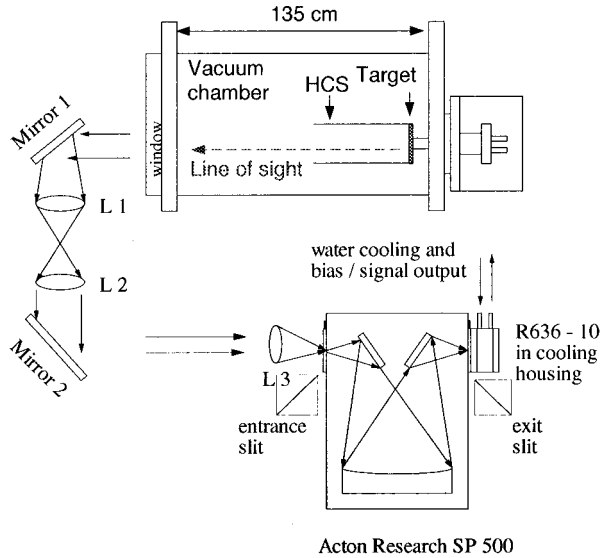

FIG. 2. Schematic of the optics setup for the N energy distribution measurement.

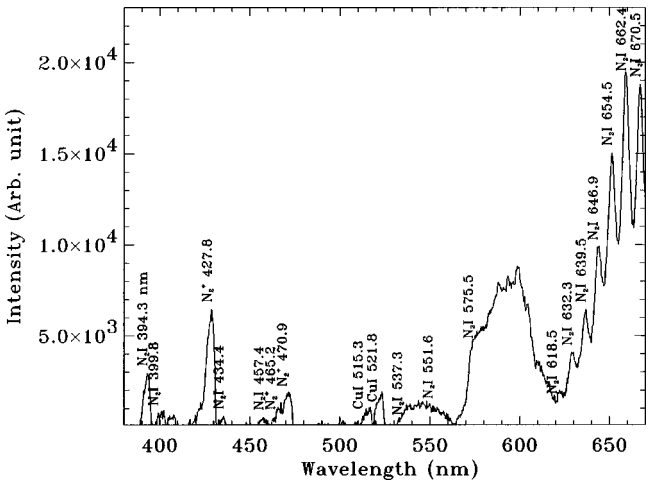

FIG. 3. Nitrogen discharge spectrum from 380 to 670 nm.

measured to be 0.07 nm. (The measured line showed a Gaussian shape.) This corresponds to an instrumental temperature of 17.1 eV for nitrogen. (The same line had a width of 0.02 nm when measured with a Fabry-Perot spectrometer.) We note that the primary mechanism for line broadening in the HCPM is the Doppler effect. The Zeeman and Stark effects are relatively unimportant at the low magnetic field and plasma density of these experiments [9].

Post-processing of PMT signals was done in several steps: (1) preamplification and conversion of current signals to voltage signals; (2) integration of the voltage signals; (3) digitization of the analog voltage signals; (4) storage of the digitized signals in a memory module. The spectrometer grating, data acquisition and processing system were properly timed by a Power Mac 7100 using LabVIEW.

III. RESULTS

The spectra can be analyzed in two steps. First one can look at the spectra as a whole, i.e., the area under the spectral line, to examine the population of N atoms. This includes both thermal atoms and hyperthermal atoms. Because, as will be shown below, the thermal population is significantly larger than the hyperthermal population, the spectral line area can be used as a measure of the thermal population. In the second step, the detailed shapes of the spectra will be analyzed to determine and examine the fraction of the spectra ($<1\%$) that corresponds to the hyperthermal component.

Correspondingly, there are two parts to this section. Part A presents results that are obtained in a straightforward analysis of the raw data. It first presents the overall spectrum from the plasma and the identification of a suitable N *I* line. It then describes the dependence of the peak emission on plasma current and gives a temperature by which to characterize the cool, c. <10 eV, N atoms. That energy could arise from Franck-Condon dissociation of nitrogen molecules or be part of the slowing-down spectrum of faster neutrals created by backscattering of energetic ions. Part B presents analyzed data, obtained via a very powerful deconvolution method described in some detail in the Appendix and in great detail in the Refs. [10,11]. This refinement allows determination of the N atom velocities, rather than simply temperature. In part B we also extend the analysis to larger Dop-

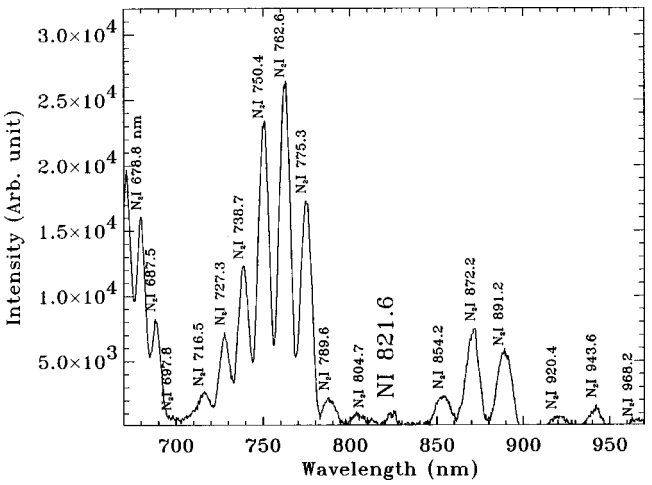

FIG. 4. Nitrogen discharge spectrum from 670 to 970 nm.

pler shifts, hence to more energetic particles.

A. Bulk atom emission intensity and temperature

Figures 3 and 4 show the observed spectrum (670–970 nm and 370–670 nm) for a N_2 HCPM plasma with 190 mA cathode current and 407 volt cathode bias. Of the ~40 spectral lines labeled, only one (group), at 821.6 nm, is due to atomic N. The others are primarily due to N_2. A few lines attributable to sputtered copper are also visible. (For a H_2 plasma, a spectral scan with identical sensitivity and resolution over the same wavelength region did not reveal any bright atomic lines sufficiently separated from molecular emission to allow a useful study.) A higher-resolution spectral scan of the N_2 plasma is shown in Fig. 5 for the spectral region 810–830 nm. All these lines are due to N I [13]. The 821.6-nm line, due to the transition $3p4P \rightarrow 3s4P$ ($J' = {}^3D_{5/2} \rightarrow J = {}^3D_{5/2}$), is chosen for most analyses since it is the brightest. Note that the nearest lines are +6.8 Å and −5.6 Å away. Energywise, these lines would correspond to a Doppler shift for N atoms of about 4 keV, which is well

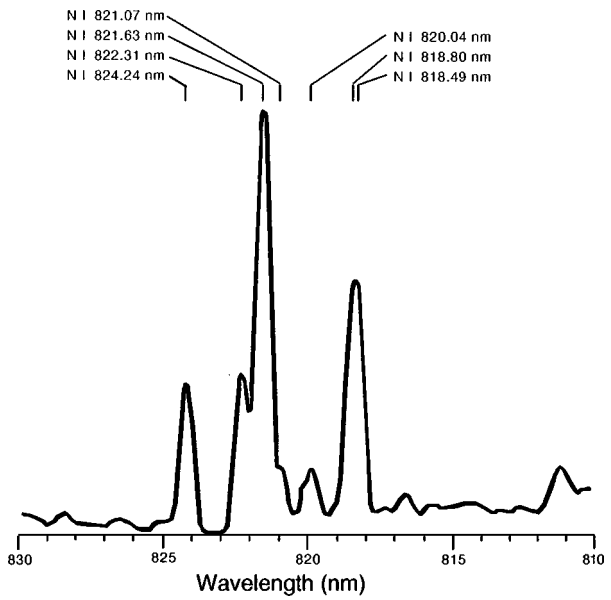

FIG. 5. Nitrogen atomic lines around N I 821.6 nm.

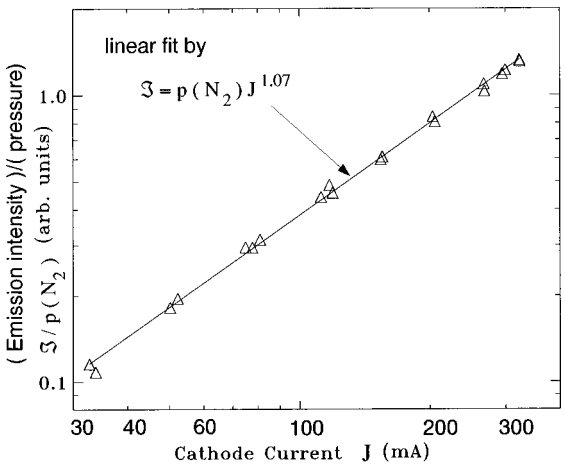

FIG. 6. N I 8216-Å lines' intensity of dependence on cathode current J.

beyond the experimental cathode bias of up to −1500 V. Hence these neighboring N lines do not contaminate the spectra we obtained.

Following Rossnagel and Saenger [14] or Gau and Lieberman [15], the intensity of the N I 8216.3 Å as a function of total cathode current was measured; see Fig. 6. This is to elucidate the source of the nitrogen atoms responsible for the peak of the emission from the N I 8216.3 Å line. (Intensity here means the line's peak value.) Data shown are for different N_2 pressures $p(N_2)$ ranging from a few mTorr to about 100 mTorr. From the fitting shown, we see that the emission intensity I is proportional to background pressure $p(N_2)$ and cathode current J to the first power. (The peak intensity includes only a small contribution from energetic neutral particles because of their large Doppler shift.)

$$\mathrm{Im} = p(N_2) \times J. \tag{1}$$

Figure 7 shows Doppler broadening of the 8216.3-Å line at different pressures, in comparison with the instrumental profile. A blue-red asymmetry is seen. Accordingly, we define two temperatures, a blueshifted and a redshifted, each represented by a half-Gaussian. The (blue or red) bulk N temperature T_0 was obtained by subtracting the raw data

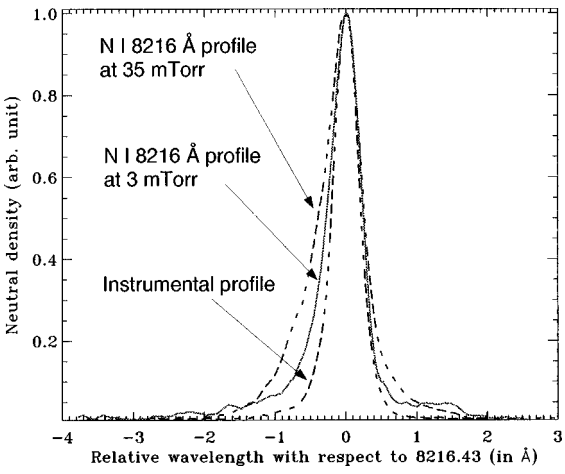

FIG. 7. Comparison of the raw data of the N I 821.6-nm profiles with instrumental profile. Blue and red asymmetry is observed.

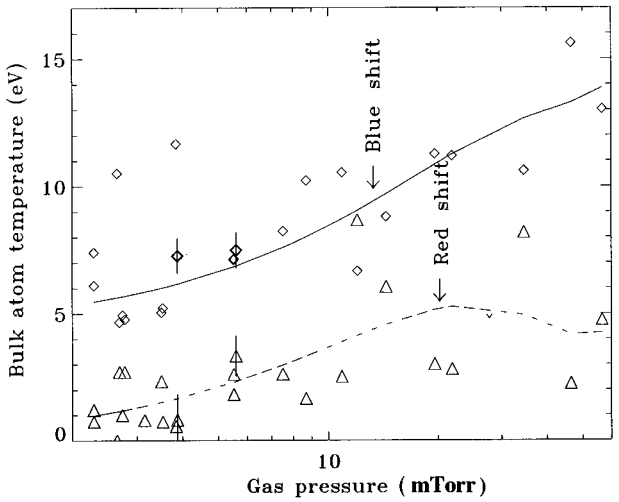

FIG. 8. Bulk N temperature as a function of pressure. The error bars shown are typical.

temperature T_s which is proportional to (the square of) the full width at half-maximum (FWHM) from the instrumental T_I:

$$T_0 = T_s - T_I . \tag{2}$$

As a function of discharge pressure, the blue and red bulk N temperatures are shown in Fig. 8. The asymmetry is clear, with the blueshifted (forward-moving) N atoms being warmer than the redshifted. (The blueshifted atoms are also about 5 times brighter than the redshifted.) The bulk temperatures increase with pressure. Figure 8 shows bulk N atom temperatures in the range 1–15 eV, increasing as the pressure is increased. The temperature on the blueshift side is always greater than that on the redshift side. The magnitude of the temperature is understandable in a qualitative fashion. The formation of neutral N atoms with these low energies proceeds primarily by Franck-Condon dissociation of N_2. The energy of Franck-Condon neutrals depends on electron energy. For example, at low electron energies, c. 20 eV, the main process is via excitation from the $X^1\Sigma_g$ state to the autodissociating $C^3\Pi_u$ state, creating N atoms in the range 1.4–4.4 eV [16]. Higher-energy electrons can promote excitation to autodissociating states that produce more energetic electrons, to ~10 eV. Randomization of the Franck-Condon energy produces a temperature equal to approximately half of the energy, consistent with the low-pressure data of Fig. 8. The asymmetry of the temperatures may be due to collisions with sputtered atoms or backscattered impacting ions.

B. N atom energy distribution

First consider the possibilities for spectral distortion. The optical depth for the 8216-Å line is $\tau \sim 0.02\ \mathrm{cm}^{-1}$ assuming a N density of $10^{10}\ \mathrm{cm}^{-3}$ (upper limit) and a N temperature of 1 eV (lower limit), based on Griem's result [12]. The plasma dimension is about 1–5 cm. Distortion of the spectra (lineshape) due to absorption is thus negligible because the plasma is optically thin at the line center, and even more so at the wings.

There was no view dump possible for this type of line-integrated measurement. Lineshape distortion due to reflection of light from the metallic hollow cathode may occur. Experimental data (see Figs. 9 and 11) show more intense blueshift light than redshift light. The most straightforward explanation for this asymmetry is that there is a net particle flow towards the detector, away from the cathode. But because the cathode is a reflective surface for visible light, the redshift signal could be due to either particles moving towards the cathode or the reflection of light from energetic N atoms that emit light back towards the cathode while moving away from it. We have compared the intensity of the redshift side to that of the blueshift side for Figs. 9 and 11. For the measured asymmetry to be due to reflectivity, the surface would have to specularly reflect 30–40 % of the light, assuming that N has equal probability of emitting a photon towards the detector and away from the detector. We have measured the reflectivity of a copper cathode after removal from the system. Typical values are 1–2 %, with a maximum of 5%.

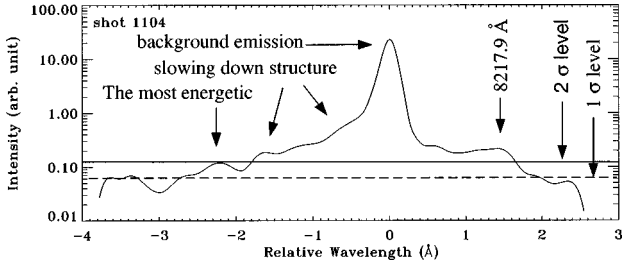

FIG. 9. N I 8216-Å line profile for $p = 2.74$ mTorr, $V_b = -1114$ V, and $J = 279$ mA; W target.

Besides light emission by energetic N, the only other contribution is that energetic N ions (moving away from the detector) exchange charge with cold N atoms. The resulting energetic N then will emit Doppler-shifted light. However, energetic N ions exist only within the cathode sheath. We estimate that charge exchange is not important for pressures less than 10 mTorr.

With high-Z (tungsten, W) and low-Z (aluminum, Al) targets, the spectra near the N I 8216 Å line were obtained along a view that is perpendicular to the surface of the target, as shown in Fig. 1. High and low gas pressures were studied (Figs. 9–12). The following discussion is based on the deconvolved data, the solid line in each figure. The raw data are corrected due to the inverse square-root dependence of the line intensity on the particle energy.

Fig. 9 is obtained for a 279-mA HCPM discharge, with a cathode bias of −1114 V, above a W target at a N_2 pressure of 2.74 mTorr. (A pressure less than five mTorr is in the low-pressure regime defined in our earlier experiments.) The

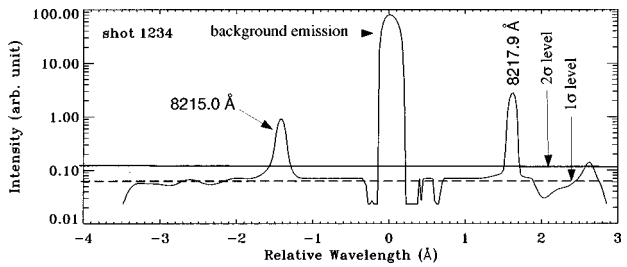

FIG. 10. N I 8216-Å line profile for $p = 4.38$ mTorr, $V_b = -369$ V, and $J = 312$ mA; Al target.

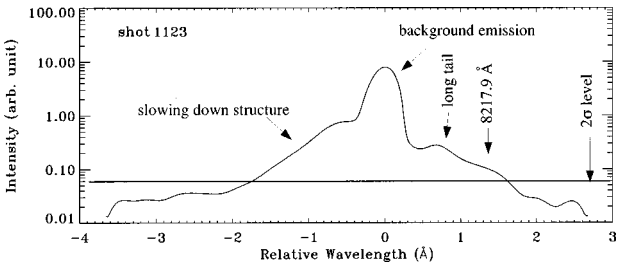

FIG. 11. N I 8216-Å line profile for $p=34.5$ mTorr, $V_b=-570$ V, and $J=295$ mA; W target.

peak intensity at N I 8216 Å is over a 100 times stronger than the peak intensity a few Å away. The peak of the emission line profile (labeled as background emission in Fig. 7) is due to the cool N atoms just discussed, those with up to a few eV in energy, and with a Doppler shift $\leqslant 0.4$ Å.

The 1σ level (straight dashed line in the figure) is the noise level, defined as the average signal level (of the smoothed curve) towards the outer wings (left and right) of the line peak. The noise level is determined by the sum of the electronics noise, amplifier noise, digitizer noise, background light emission, etc. Signals at twice the noise level, the 2σ level (solid straight line in Fig. 7), have about an 80% statistical likelihood of being due to N-atom emission.

The deconvolved signal exceeds the 2σ level from the peak out to a relative wavelength of about -2 Å in the blueshift direction and to $+1.6$ Å in the redshift direction. The peak at a -2.2 Å shift in wavelength would arise from N atoms having an energy of about 475 eV. These are the most energetic N atoms, according to the spectral line profile, and are labeled as such in Fig. 9. The region between -1.8 Å and the peak is labeled in Fig. 9 as the *slowing-down structure*. The slowing-down structure will be discussed in more detail later. A small but interesting feature, labeled as 8217.9 Å, is noted. Its interpretation as a spectral line is discussed after consideration of spectra obtained with an Al cathode.

Figure 10 is a data set for an Al cathode at low pressure, 4.38 mTorr. Besides having a lower Z value compared with the W cathode case, the cathode bias of the HCPM, -369 V, is much smaller than the -1114-V bias used for the W cathode. Similarly to Fig. 9, the background emission due to cold N atoms is about 100 times more intense than the rest. Compared with Fig. 9, we see above the 2σ level only three sharp spectral structures, but no extended slowing-down structure. The power of Jansson's deconvolution method is clear as it reveals sharp spectral features at 8217.9 ± 0.1 Å and 8215.0 Å. The wavelengths of the deconvolved lines shown are not affected by choice of the deconvolution parameters. The

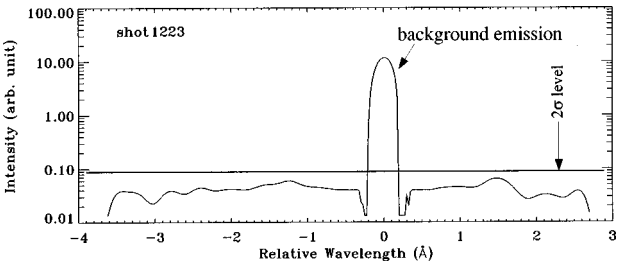

FIG. 12. N I 8216-Å line profile for $p=30.4$ mTorr, $V_b=-339$ V, and $J=256$ mA; Al target.

8217.9 Å feature appears in Fig. 9, just above the 2σ level. Furthermore, its existence and location were found to be independent of cathode bias. Therefore, we identify it as a spectral line instead of relating it to Doppler-shifted N I 8216 Å. Further discussion of the dependence of energy spectra on cathode bias is given later. This line at 8217.9 Å may be a nitrogen line, because its existence does not depend on target material. However, we have not found a nitrogen atom or ion line at this wavelength listed in the standard spectral tables. The origin of the other sharp spectral feature, at 8215.0 Å, is also not clear. These two spectral features are not due to sputtered W atoms, according to the spectral line tables [13]. Other possibilities for these unknown lines could be impurities in the wall material or impurity in the nitrogen gas used for these experiments. We failed to identified 8215.0 Å as an argon I line, because its intensity did not increase with Ar pressure. For the Al cathode, the deconvolved spectrum in Fig. 10 shows very little light between -0.2 and -1.2 Å.

Figure 11 is for a W cathode at higher gas pressure, 34.5 mTorr, and lower cathode bias, -570 V. Again, a slowing-down structure is identified, but extends to only -1.8 Å. For N atoms, this Doppler shift corresponds to 316 eV. Again the long tail at the redshift side is seen. The redshifted long tail and the blueshifted slowing-down structure can be fit by a shifted-Maxwellian distribution with a temperature on the order of 50 eV. Again, the spectral line 8217.9 Å shows up.

The deconvolved spectrum in Fig. 12, for the Al target, also at higher pressure (30.4 mTorr) and lower voltage (339 V) shows a simple structure. Only emission near the peak is above the 2σ level.

In the following section we convert the spectra into energy distributions and compare them with a numerical model of scattering, VFTRIM.

IV. DISCUSSION

From energy considerations, the mechanism for generating energetic neutral atoms (with more than 50 eV) in the HCPM must be related to ions colliding with the cathode surface. Ions are produced in the plasma by electron impact and have initial energy V_0 less than a few eV. Futhermore, only a small electric field exists within the plasma. It is when ions fall through the cathode sheath, in the absence of collisions, that they gain appreciable energy, equal to the full cathode bias V_b. Therefore, the upper limit energy E_i when these ions strike the cathode surface is

$$E_i = V_b + V_0 \simeq V_b . \tag{3}$$

An energetic ion can be reflected as a neutral particle, retaining a substantial fraction of its incidental energy. The energy retained depends on ion species, the cathode material, lattice structure, incidental angle, and incident ion energy, as well as the number of collisions this ion experiences as it transverses the plasma.

For plasma discharges involving molecular gases, such as N_2, the ions involved can be atomic ions N^+, or molecular ion $N_2{}^+$. We can conceive of three distinct sequences by which energetic atomic neutrals may be produced.

(1) From N^+ ions. A N^+ hits the cathode surface, reflected as an energetic nitrogen atom N_E.

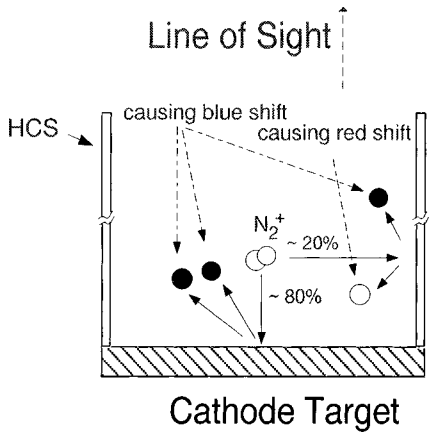

FIG. 13. Blue and red shift are due to the ion collisions with the HCPM cathode at different locations.

(2) From N^+ ions. A N^+ hits the cathode surface, reflected as energetic $N_E{}^-$. The N_E- undergoes a second acceleration through the sheath, N^- exchanges charge with a cold N, and becomes a N_E:

$$N_E{}^- + N \rightarrow N_E + N^- . \tag{4}$$

(3) From $N_2{}^+$ ions. A $N_2{}^+$ strikes the cathode surface, undergoes dissociative neutralization, and is reflected as two N_E's:

$$N_2{}^+ + e_s \rightarrow 2N_E . \tag{5}$$

e_s means an electron from the surface. We propose the third process as the main process for energetic N atom generation in our experimental conditions. The reasons are the following.

The energy required to break the bond between the two N's in a $N_2{}^+$ is around 9 eV. According to Winter and Horne [17], the probability of a $N_2{}^+$ dissociating into 2 N atoms depends on the incident $N_2{}^+$'s energy when it is reflected from a metallic surface. For energies greater than 100 eV (much greater than the bond energy of 9 eV), the dissociation probability reaches unity for W, Ni, and Mo targets. Our experimental conditions guarantee that all $N_2{}^+$'s hitting the $N_2{}^+$'s cathode surface have energy above 100 eV. All the $N_2{}^+$'s dissociate as two N atoms when they are reflected by the cathode.

The reflection energy peak as a function of cathode bias at low pressures (Fig. 15) showed that the maximum energy carried by energetic atoms is less than 50% of the total incidental energy of the ion (that is, the cathode bias). This is consistent with the proposition that the total incidental energy of any $N_2{}^+$ ion is equally distributed between two energetic N atoms generated in the dissociation process.

Finally, as suggested by the full visible range plasma emission spectra analysis, the largest fraction of ions in the discharges is $N_2{}^+$ under our experimental conditions. The N^+ ions are far fewer than $N_2{}^+$ within the discharge. Even though N^+ ions do produce energetic N atoms, their signal is probably too small to be measured by the detector used.

It is speculated that of the cause of the red-blue asymmetry is the interaction between the Franck-Condon neutrals and the backscattered energetic N atoms. (The sputtered cathode atoms may play a small role.) As shown in Fig. 13, in a HCPM plasma bombards the HCS side walls, as well as the planar region. At a pressure of 1 mTorr, the mean free path for energetic N atoms backscattered from the cathode is about 10 cm. Hence, even at the lowest pressures of our experiments, collisions between backscattered N and the Franck-Condon N population will transfer momentum to the Franck-Condon neutrals. Because the majority (70–90 %) of the ions hit the planar cathode, the Franck-Condon distribution will preferentially drift towards the optics, creating a blueshift in their emitted light.

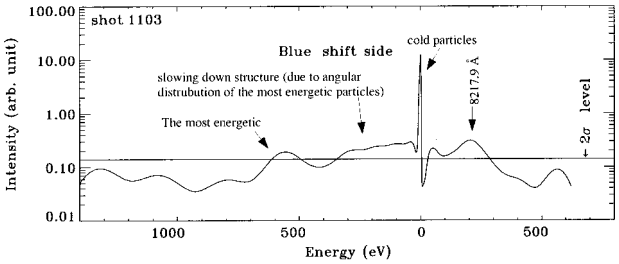

FIG. 14. N energy distribution for $p = 2.29$ mTorr, $V_b = -1281$ V, and $J = 281$ mA; W target.

Two effects can contribute to the redshift. First, 10–30 % of the ions hit the hollow cathode structure. When these backscatter they can provide momentum either toward or away from the optics. Second, the proximity of the walls allows collisions of the Franck-Condon neutrals with them. This will redistribute some of the energy to the redshifted direction.

Based on Figs. 9–12, energetic N's arise from reflection from the W cathode. We have studied the energy distribution of N with a W target at various pressures. In Figs. 14 and 15, the Doppler shift of the N I 8216 Å line has been converted into an energy unit (eV), i.e., as an energy distribution.

Compare N energy distribution for two pressures: $p = 2.29$ mTorr (Fig. 14) and $p = 56.7$ mTorr (Fig. 15). The most energetic N atoms for $p = 2.29$ mTorr have energies around 600 eV (Fig. 14), while the most energetic N atoms for $p = 56.7$ mTorr have energies about 300 eV (Fig. 15). Such a difference is correlated with the different cathode biases: $V = -1281$ V in Fig. 14 and $V = -554$ V in Fig. 15. The VFTRIM results will support this connection.

There are two possible causes of a slowing-down structure: (i) most of the energetic particles going sideways with respect to the sight of observation (these are *pseudo*-slowing-down particles because only the velocity component along

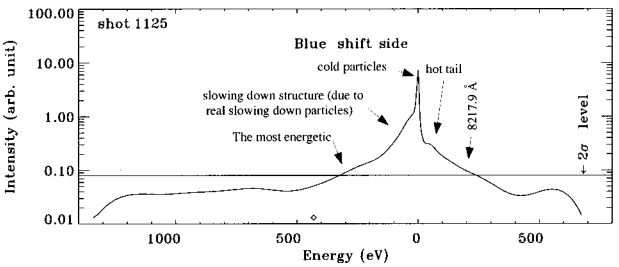

FIG. 15. N energy distribution for $p = 56.7$ mTorr, $V_b = -554$ V; and $J = 299$ mA; W target.

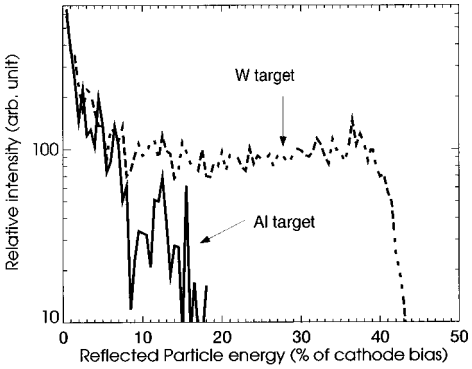

FIG. 16. Example of reflected N energy peak as a function of cathode bias for $p=2.45$ mTorr, $V_b=-1288$ V; $J=337$ mA, and W target.

the line of sight of observation was detected); (ii) particles with less energy (these are the *real* slowing-down particles). From the mean-free-path considerations, even at low pressures collisions are important because of the HCS.

One way to discriminate between these two causes of the slowing-down structure is to look at the bulk particle temperature, determined by the width of the line peak. The bulk particle temperature is higher at higher pressure. Indicating that true slowing down is occurring.

We now compare the measured maximum reflected N energy with VFTRIM simulations. Figure 16 shows typical VFTRIM simulation results for N collision with W (1200-V bias) and Al cathode (400-V bias). For Al cathode, reflected N's retain up to 16% of the incident energy. For W cathodes, N's retain about 40% of the total incidental energy. For an Al cathode bias of about -400 V (similar to the experimental conditions), VFTRIM predicts less than 70 eV for each reflected N atom. This VFTRIM prediction is consistent with the deconvolved data shown Figs. 10 and 12. VFTRIM predicts about 500 eV reflected N for a -1200-V W-cathode bias. The most energetic N observed was about 589 eV (Fig. 17. This difference is only partly explained by the experimental error bar, as shown later in Fig. 19.

One detailed comparison of the VFTRIM results with experiment is shown for plasma shot No. 1103 in Fig. 18. Figure 19 summarizes the maximum experimental reflected N energy (in fraction of the bias) for a W cathode at different cathode biases. VFTRIM predicts a constant fraction for maximum reflected energy, while the experiment shows an increasing fraction with energy. A similar trend was also observed by Cuthbertson *et al.* [1] for atom collisions with

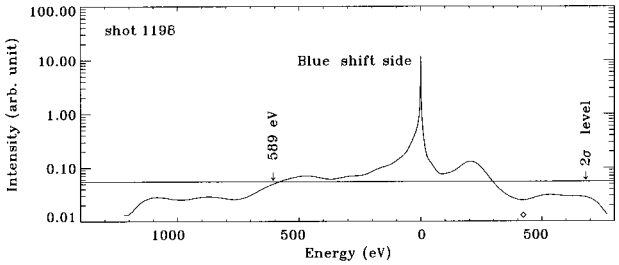

FIG. 17. An example of the VFTRIM prediction of the reflected N energy distribution for a W cathode (dashed curve) and a Al cathode (solid curve).

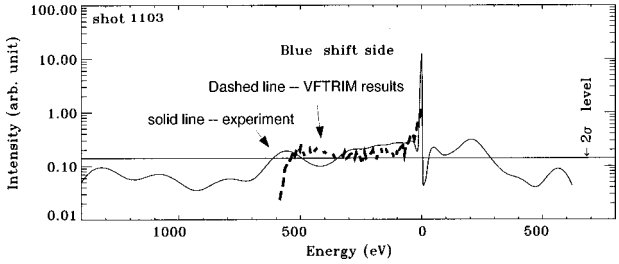

FIG. 18. Detailed comparison of experimental N energy distribution with VFTRIM prediction under similar conditions; W cathode.

metal surfaces. The observed reflection energy peaks are less than 50% of the total N_2^+ incidental energy onto the cathode. For comparison, the result using a simple binary collision model (N-W atom collision) which predicts that the reflected energy (E_{ref}) and the cathode bias (V_b) ratio is determined by the W atom mass (M_W) and N atom mass (M_N):

$$\frac{E_{ref}}{V_b}=\frac{1}{2}\frac{M_W-M_N}{M_W+M_N}=43\%. \tag{6}$$

This prediction is more than that of VFTRIM (about 37%). It agrees with experiment in the high energy (>1 kV) end, which might suggest that for high-energy N-W cathode collisions, the binary collision mechanism is important [1]. Because the molecular bonding energy is small in comparison with cathode bias, a biatomic ion collision with the cathode is similar to that of two atoms colliding with the cathode independently, hence the factor 1/2 on the right-hand side of Eq. (6).

The VFTRIM code simulates particle-surface interaction pretty well in many cases. VFTRIM simulations do not include particle transport through the plasma and gas, which is particularly important for p>13 mTorr. VFTRIM coupling with some plasma code that simulates transport of particles within the plasma could be more useful in a comparison with the experimental data presented here.

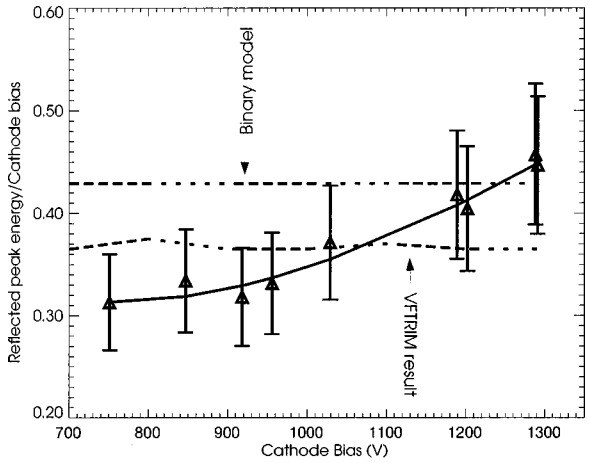

FIG. 19. Peak reflection energy (in fraction of total cathode bias) vs the cathode bias for a W target. VFTRIM results are plotted in the dashed line. Also shown is the binary model result (solid line), as explained in text.

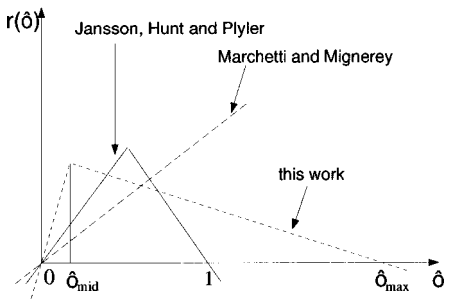

FIG. 20. Relaxation function $r(O)$ used for this work, in comparison with Jansson's classic $r(O)$ and the one by Marchetti and Migerey [18] for emission spectra.

ACKNOWLEDGMENTS

We are grateful to Mr. B. Berlinger and Mr. T. Bennett for their technical help. This work was supported by U.S. DOE through Contract No. DE-AC02-76-CHO-3073.

APPENDIX

Jansson's deconvolution method is mathematically described by the iteration process

$$O^{k+1}=O^k+r(O)\times(i-S\otimes O^k). \tag{A1}$$

In the above, O is the deconvolved spectrum, i is the raw data/spectrum, S is the instrumental function, k is the kth step, and $k+1$ is the $(k+1)$th step. To start with, $O^k=i$. $\otimes$ stands for convolution. $r(O)$ is called the relaxation function. We have used a generalized $r(O)$ in this work: a generalized relaxation function that includes Jansson's original $r(O)$ [10] and the one used by Marchetti and Migerey [18] as special cases is

$$r(O)=\begin{cases}\kappa_0 O, & \text{if } O\leqslant O_{mid},\\ \kappa_0 O_{mid}\dfrac{O-O_{max}}{O_{mid}-O_{max}}, & \text{for } O\geqslant O_{mid}.\end{cases} \tag{A2}$$

Optimal values are found for $\kappa_0>0$, O_{mid} and O_{max} using the minimization of χ_w^2 criterion. χ_w^2 is defined as $(O\otimes S-i)^2$ with a weight factor that is proportional to $1/i$. A comparison of this relaxation function to Jansson's [10] and Marchetti and Migerey's [18] is shown in Fig. 20. The deconvolution technique [basically identifying a proper $r(O)$ and the number of steps of iteration] is described elsewhere in more detail [10,11].

[1] J.W. Cuthbertson, W.D. Langer, and R.W. Motley, J. Nucl. Mater. **196-198**, 113 (1992).
[2] W. Eckstein, *Computer Simulation of Ion-solid Interations* (Springer-Verlag, Berlin, 1991).
[3] Z. Wang and S.A. Cohen, J. Vac. Sci. Technol. A **17**, 77 (1999).
[4] K.S. Fancey, and A. Matthews, Vacuum **43**, 1013 (1991).
[5] F. Guimarães, J.B. Almeida, and J. Bretagne, Plasma Sources Sci. Technol. **2**, 138 (1993).
[6] D.N. Ruzic, and H.K. Chiu, J. Nucl. Mater. **162-164**, 904 (1989).
[7] Z. Wang and S.A. Cohen, Phys. Plasmas **6**, 1655 (1999).
[8] *Thin Film Processes*, edited by J.L. Vossen and W. Kern (Academic Press, New York, 1978).
[9] M.J. Goeckner, J. Goree, and T.E. Sheridan, J. Vac. Sci. Technol. A **8**, 3920 (1990).
[10] *Deconvolution of Images and Spectra*, edited by P.A. Jansson (Academic Press, New York, 1997), Chap. 4.
[11] Z. Wang, Ph. D thesis, Princeton University, 1998.
[12] H.R. Griem, *Plasma Spectroscopy* (Academic Press, New York, 1966), p. 198.
[13] A.N. Zaidel, V.K. Prokof'ev, S.M. Raiskii, V.M. Slavyni, and E. Yu. Shreider, *Tables of Spectral Lines*, (IFI/Plenum, New York, 1970).
[14] S.M. Rossnagel, and K.L. Saenger, J. Vac. Sci. Technol. A **7**, 968 (1989).
[15] L. Gau and M.A. Lieberman, J. Vac. Sci. Technol. A **6**, 2960 (1988).
[16] J.T. Fons, R.S. Schappe, and C.C. Lin, Phys. Rev. A **53**, 2239 (1996).
[17] H.F. Winter and D.E. Horne, Surf. Sci. **24**, 587 (1971).
[18] A.A. Marchetti and V.A. Migerey, Nucl. Instrum. Methods Phys. Res. A **324**, 288 (1993).